

# Performance Analysis of a Joint Space-Time Block Codes and Channel Estimation Scheme in DL-PUSC Mode of Mobile WiMAX.

Phuong T.T. Pham, and Tomohisa Wada

Information Engineering Department, Graduate School of Engineering and Science,  
University of The Ryukyus, 1 Senbaru Nishihara, Okinawa, 903-0213, Japan.  
thuphuong@lsi.ie.u-ryukyu.ac.jp, wada@ie.u-ryukyu.ac.jp

**Abstract.** Mobile WiMAX has emerged as a starting point of broadband mobile wireless era. Besides plenty of advantages over the prior systems, it also utilizes multiple-antenna techniques to improve the transmission quality. Although this approach has been intensively studied, there are just few published works taking into account channel estimation to obtain realistic performance. This paper studies a joint STBC and channel estimation scheme to investigate the performance of the DL-PUSC mobile WiMAX in various mobile channels. Simulation results show significant improvement, up to 8 dB gain for PER and system throughput is achieved when employing STBC.

**Keywords:** WiMAX, DL-PUSC, MIMO, Alamouti, MRC, Channel estimation.

## 1 Introduction

The IEEE 802.16e standard, often commercially regarded as mobile WiMAX (Worldwide interoperability for Microwave Access), is a stimulating technology that provides wireless access over large coverage area with high speed, high throughput and full mobility. WiMAX physical layer utilizes advanced multiple access scheme called scalable OFDMA (Orthogonal Frequency Division Multiple Access) which is derived from OFDM (Orthogonal Frequency Division Multiplexing) technique. OFDM is well known to be very efficient in utilizing the system bandwidth as well as mitigating the impairment caused by multipath frequency-selective fading channel. OFDMA multiplexes data streams from different individual users by subchannelizing the OFDM symbol and assigning each user a group of subchannels. Permuting these subchannels together, this technique can guarantee that none of the users has higher probability to suffer the severely faded channel than others. Implemented scalability supports a flexible operating bandwidth from 1.25 MHz to 20 MHz by varying the FFT size from 128 to 2048. This advantage is very important since it increases the spectral efficiency which is critical in broadband wireless network.

DL-PUSC (Downlink - Partial Usage of Subchannels), which is a particular working mode defined in [1], has received lots of interest for evaluating the system performance. This subchannelization mode assigns each user a group of subchannels consisting of several clusters. Clusters of a user are pseudo-randomly permuted

among those of other users so that the system can take advantage of the frequency diversity to compete the fading channel.

Recently, the technique using multiple antennas at the transmitter and receiver called MIMO (multiple input – multiple output) has received a growing expectation to be applied to the upcoming wireless networks. MIMO technique exploits the spatial diversity to provide a significant improvement in system performance over the traditional SISO (single input – single output) approach [2]. MIMO is mainly implemented in three ways, i.e. maximizing the spatial diversity to enhance the power efficiency, increasing the capacity by using layered approach and the last one exploiting the channel knowledge feedbacked from the receiver to decompose the channel coefficient matrix by singular value decomposition [3]. Although the last scheme is proved to be able to reach the near Shannon capacity, the first one which includes several techniques such as delay diversity, space-time trellis codes, and space-time block codes (STBC) is more mature to be applied widely to practical systems. Has been vastly studied [4]-[11], STBC including the well known Alamouti scheme is one of the diversity techniques recommended by the IEEE 802.16e standard for WiMAX systems.

This paper studies applying several MIMO-STBC techniques such as maximal ratio combining (MRC), 2x1-, and 2x2- Alamouti schemes to the mobile WiMAX DL-PUSC system. Channel estimation using conventional linear interpolation technique [12] is carried out by exploiting scattered pilots in clusters rather than assuming perfectly known to obtain more practical results. Performance analysis is presented in term of packet error rate (PER) and system throughput versus signal to noise ratio (SNR) in various frequency selective fading channels. These channel models are recommended by ITU [13] for low-speed and high-speed mobile environments. Performance comparisons with SISO approach are given to show the improvement when applying MIMO techniques to the system.

In this paper, a capital letter is used to denote a frequency domain symbol, bold letter is used for a matrix or a vector whereas indexing symbol is written in italic subscript, and a ranging number is in italic capital form.

The rest of the paper is organized as follows. A brief description about DL-PUSC is given in section 2. Conventional SISO approach is introduced in section 3. MIMO-STBC including maximal ratio combining, 2x1-, and 2x2- Alamouti schemes are addressed in section 4. Channel models, simulation setup, simulation results, and discussions are presented in section 5. Finally, section 6 reviews the main aspects and concludes the paper.

## **2 System Overview**

### **2.1 DL-PUSC Structure**

The data structure in DL-PUSC mode is shown in fig. 1. The OFDM symbol is divided into subchannels, each user is associated to a group of subchannels. Subchannel is further partitioned into clusters and each of which contains a group of

14 consecutive subcarriers. When transmitted, clusters of different users will be permuted among themselves.

Pilot pattern in DL-PUSC is assigned cluster by cluster and designed periodic in 2-symbol period. The first symbol that carries data is considered as even and has index 0. In each cluster, pilots are arranged at subcarriers {4,8} for even symbols and at subcarriers {0,12} for odd symbols.

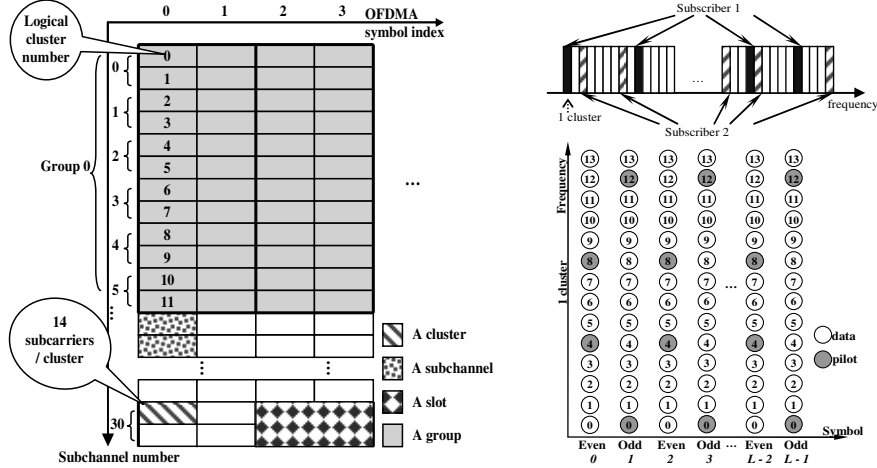


**Fig. 1.** Basic elements in DL-PUSC mode (left); Clusters permutation in OFDM symbol (upper right); Pilot pattern (lower right).

## 2.2 Signal Model

A general OFDM-MIMO transmission scheme is shown in fig. 2 in which there are  $N$  and  $M$  antennas at the transmitter and receiver respectively. In case of using SISO, the Tx diversity encoder is omitted, the channel equalizer is used instead of the Rx diversity combiner and just only one IFFT/FFT block and antenna appear at the transmitter and receiver.

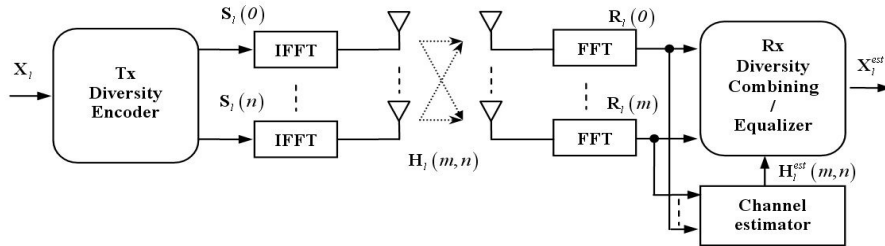


**Fig. 2.** Transceiver diversity OFDM system

Suppose at symbol-period  $l$ , processed OFDM symbols set  $\{S_i(n)\}$  are transmitted from the base station with all transmit (Tx) antennas to the mobile station. At the  $m^{\text{th}}$  receive (Rx) antenna, after FFT, the received symbol is:

$$\mathbf{R}_l(m) = \sum_{n=0}^{N-1} \mathbf{H}_l(m,n) \mathbf{S}_l(n) + \mathbf{W}_l(m) . \quad (1)$$

where  $\mathbf{H}_l(m,n)$  is the frequency response of the channel between the  $n^{\text{th}}$  Tx antenna to the  $m^{\text{th}}$  Rx antenna,  $\mathbf{W}_l(m)$  is the noise at that Rx antenna,  $n = 0, 1, \dots, N-1$ ,  $m = 0, 1, \dots, M-1$  with  $N$  and  $M$  are the numbers of Tx and Rx antennas respectively.

In subcarrier-scale, these vectors are defined as follows.  $\mathbf{R}_l(m) = [\mathbf{R}_0(m), \mathbf{R}_1(m), \dots, \mathbf{R}_{K-1}(m)]_l^T$ ,  $\mathbf{H}_l(m,n) = [\mathbf{H}_0(m,n), \mathbf{H}_1(m,n), \dots, \mathbf{H}_{K-1}(m,n)]_l^T$ ,  $\mathbf{S}_l(n) = [\mathbf{S}_0(n), \mathbf{S}_1(n), \dots, \mathbf{S}_{K-1}(n)]_l^T$ ,  $\mathbf{W}_l(m) = [\mathbf{W}_0(m), \mathbf{W}_1(m), \dots, \mathbf{W}_{K-1}(m)]_l^T$  in which  $[\cdot]^T$  is matrix transpose operator and inside brackets are the correspondent values at the  $k^{\text{th}}$  subcarrier of the  $l^{\text{th}}$  OFDM symbol,  $k = 0, 1, \dots, K-1$  with  $K$  is the number of subcarriers in OFDM symbol, whereas  $l$  can take any value between 0 and  $L-1$ ,  $L$  is even and denotes the number of symbols in the transmission frame.

The transfer function of the channel from Tx antenna  $n$  to Rx antenna  $m$  at the  $l^{\text{th}}$  symbol-period is the Fourier transform of the channel impulse response  $\mathbf{H}_l(m,n) = \mathbf{F} \mathbf{h}_l(m,n)$ , where  $\mathbf{F}$  is the  $K \times I$  – Fourier transform matrix whose values are defined as  $f_{k,i} = \frac{1}{\sqrt{K}} e^{-j2\pi \frac{ki}{K}}$ , for  $i = 0, 1, \dots, I-1$ , and

$\mathbf{h}_l(m,n) = [\mathbf{h}_0(m,n), \mathbf{h}_1(m,n), \dots, \mathbf{h}_{I-1}(m,n)]_l^T$  is the  $I$ -tap discrete multipath fading channel sampled at system frequency.

In order to recover the transmitted signal, the channel transfer function must be estimated. This task is done by calculating the channel values at pilot subcarriers, which are known in advance, and interpolating all the channel values at data positions. Since the clusters of each user are not connected continuously in frequency axis, the estimation task at the receiver is carried out partially cluster by cluster. Channel should be estimated at each cluster or in a frame of several clusters connected in the time axis.

### 3 SISO Approach

In this case,  $N = M = I$ , (1) becomes

$$\mathbf{R}_l = \mathbf{H}_l \mathbf{S}_l + \mathbf{W}_l . \quad (2)$$

At pilot positions, the least square channel values can be obtained by evaluating:

$$\mathbf{H}_{k_p, l}^{LS} = \frac{\mathbf{R}_{k_p, l}}{\mathbf{S}_{k_p, l}} . \quad (3)$$

for  $k_p = \{4, 8\}$  at even symbols and  $k_p = \{0, 12\}$  at odd symbols.

Based on the pilot pattern in DL-PUSC mode, channel estimation can be performed by cascading two 1-dimension interpolations in time- and frequency-axis. Conventional linear interpolation scheme can be utilized in both time and frequency to estimate the channel transfer function. Time interpolation as shown in fig. 3 has some differences depending on the symbol (even or odd) that the cluster belongs to, whereas frequency interpolation is performed similarly for all clusters in frame since each cluster now have 4 channel values, 2 of pilots and 2 from the time interpolation.

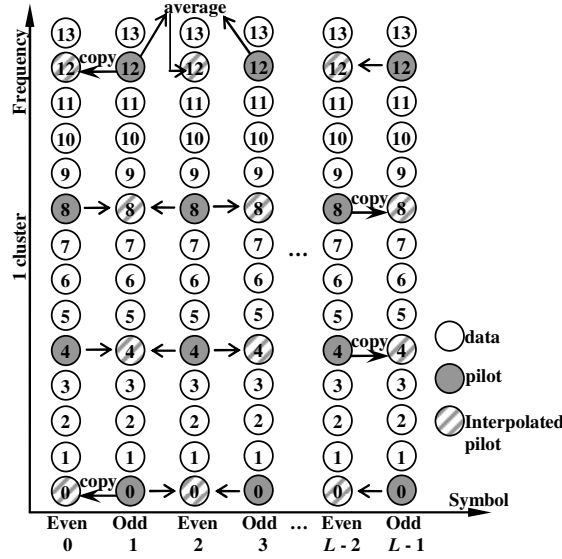


Fig. 3. Linear interpolation in time axis

*Time interpolation:*

$$\mathbf{H}_{\{0,12\},l}^{est} = \begin{cases} \mathbf{H}_{\{0,12\},l}^{LS} & l = 0 \\ \frac{\mathbf{H}_{\{0,12\},l-1}^{LS} + \mathbf{H}_{\{0,12\},l+1}^{LS}}{2} & l = 2, 4, \dots, L-2 \end{cases} \quad (4)$$

$$\mathbf{H}_{\{4,8\},l}^{est} = \begin{cases} \frac{\mathbf{H}_{\{4,8\},l-1}^{LS} + \mathbf{H}_{\{4,8\},l+1}^{LS}}{2} & l = 1, 3, \dots, L-3 \\ \mathbf{H}_{\{4,8\},L-2}^{LS} & l = L-1 \end{cases} \quad (5)$$

*Frequency interpolation:*

$$\mathbf{H}_{j,l}^{est} = \frac{\delta}{\Delta} \mathbf{H}_{k_p,l}^{est/LS} + \frac{\Delta - \delta}{\Delta} \mathbf{H}_{k_{p+1},l}^{est/LS}, \quad j = k_p + 1, \dots, k_{p+1} - 1; \quad \delta = 1, \dots, \Delta - 1, \quad (6)$$

$$\Delta = 4; \quad k_p = [0, 4, 8, 12]; \quad p = 0, \dots, 3.$$

When all the channel values are estimated, the original OFDM symbol can be recovered by equalizing:

$$\mathbf{S}^{est} = \frac{\mathbf{R}}{\mathbf{H}^{est}} . \quad (7)$$

## 4 STBC Approaches

There are 3 types of STBC recommended for mobile WiMAX system, i.e. MRC, 2x1- and 2x2- Alamouti schemes.

### 4.1 MRC ( $N = 1, M = 2$ )

In this scheme, the same OFDM symbol is transmitted from 1 Tx antenna to 2 Rx antennas. Each Rx antenna receives the data stream propagating through the channel from the transmitter to it. The received symbols at 2 Rx antennas are found as:

$$\begin{aligned} \mathbf{R}_l(0) &= \mathbf{H}_l(0,0)\mathbf{S}_l(0) + \mathbf{W}_l(0) \\ \mathbf{R}_l(1) &= \mathbf{H}_l(1,0)\mathbf{S}_l(0) + \mathbf{W}_l(1) \end{aligned} \quad (8)$$

From (8), the method to estimate the channel and recover the user's data for each stream is identical to the SISO case. Hence, two frames of  $L$  symbols are processed in parallel and then combined together to give the final data. MRC provides an effective combining scheme in which the stream corresponding to the stronger channel contributes more than the other. This approach is expressed as:

$$\mathbf{S}^{est} = \frac{\left[ \mathbf{H}(0,0)^{est} \right]^* \mathbf{R}(0) + \left[ \mathbf{H}(1,0)^{est} \right]^* \mathbf{R}(1)}{\left| \mathbf{H}(0,0)^{est} \right|^2 + \left| \mathbf{H}(1,0)^{est} \right|^2} \quad (9)$$

### 4.2 Alamouti schemes

For transmission using 2 Tx antennas, as indicated in the IEEE 802.16e standard, the cluster structure is slightly modified to meet the requirement for STBC schemes. The pilot insertion is changed so that their locations are arranged in period of 4 symbols rather than 2 symbols as before. This arrangement is shown in fig. 4. From now on, the time index  $l$  is used to denote 2 symbol periods.

Alamouti scheme uses multiple antennas at the transmitter and sends each processed symbol to the set of Tx antennas sequentially. The channels from all Tx antennas to the receiver during that time are assumed unchanged [5]. In the simulation reported below, the channels is modeled to change continuously over the simulation time rather than stay constant as assumed, but since their time variations are quite slow comparing to the symbol period, the processing formulas drawn out from this assumption are still proper.

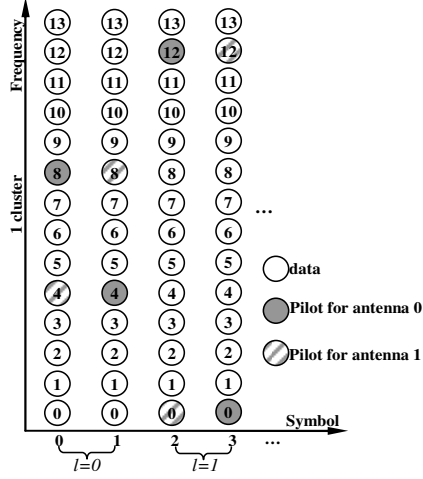


Fig. 4. Cluster structure for STBC PUSC using 2 Tx antennas

#### 4.2.1 Alamouti 2x1 ( $N = 2, M = I$ )

This scheme uses 2 antennas at the transmitter and 1 antenna at the receiver.

At symbol time  $2l$  and  $2l+1$ , the symbols transmitted at 2 Tx antennas are defined

according to the matrix  $\mathbf{A} = \begin{bmatrix} \mathbf{S}_{2l}(0) & \mathbf{S}_{2l+1}(1) \\ -[\mathbf{S}_{2l+1}(0)]^* & [\mathbf{S}_{2l}(1)]^* \end{bmatrix}$ , yielding the signal at the

receiver:

$$\mathbf{R}_{2l}(0) = \mathbf{H}(0,0)\mathbf{S}_{2l}(0) + \mathbf{H}(0,1)\mathbf{S}_{2l+1}(1) \quad (10)$$

$$\mathbf{R}_{2l+1}(0) = -\mathbf{H}(0,0)[\mathbf{S}_{2l+1}(0)]^* + \mathbf{H}(0,1)[\mathbf{S}_{2l}(1)]^*$$

The noise at the receiver in this scenario is ignored. Solving (10) at pilot subcarriers gives:

$$\mathbf{H}_{k_p,2l}(0,0) = \frac{\mathbf{R}_{k_p,2l}(0)[\mathbf{S}_{k_p,2l}(1)]^* - \mathbf{R}_{k_p,2l+1}(0)\mathbf{S}_{k_p,2l+1}(1)}{\mathbf{S}_{k_p,2l}(0)[\mathbf{S}_{k_p,2l}(1)]^* + \mathbf{S}_{k_p,2l+1}(1)[\mathbf{S}_{k_p,2l+1}(0)]^*} \quad (11)$$

$$\mathbf{H}_{k_p,2l}(0,1) = \frac{\mathbf{R}_{k_p,2l}(0)[\mathbf{S}_{k_p,2l+1}(0)]^* + \mathbf{R}_{k_p,2l+1}(0)\mathbf{S}_{k_p,2l}(0)}{\mathbf{S}_{k_p,2l}(0)[\mathbf{S}_{k_p,2l}(1)]^* + \mathbf{S}_{k_p,2l+1}(1)[\mathbf{S}_{k_p,2l+1}(0)]^*}$$

#### 4.2.2 Alamouti 2x2 ( $N = 2, M = 2$ )

The matrix  $\mathbf{A}$  is used again to arrange symbols to be transmitted at the corresponding antenna. The same approach as Alamouti 2x1 system can be derived to give the receive signals at 2 Rx antennas:

$$\begin{aligned}
\mathbf{R}_{2l}(0) &= \mathbf{H}(0,0)\mathbf{S}_{2l}(0) + \mathbf{H}(0,1)\mathbf{S}_{2l+1}(1) \\
\mathbf{R}_{2l}(1) &= \mathbf{H}(1,0)\mathbf{S}_{2l}(0) + \mathbf{H}(1,1)\mathbf{S}_{2l+1}(1) \\
\mathbf{R}_{2l+1}(0) &= -\mathbf{H}(0,0)[\mathbf{S}_{2l+1}(0)]^* + \mathbf{H}(0,1)[\mathbf{S}_{2l}(1)]^* \\
\mathbf{R}_{2l+1}(1) &= -\mathbf{H}(1,0)[\mathbf{S}_{2l+1}(0)]^* + \mathbf{H}(1,1)[\mathbf{S}_{2l}(1)]^*
\end{aligned} \tag{12}$$

By re-arranging (12) into pair of equations regarding the received signals at the same Rx antenna at symbol-time  $2l$  and  $2l+1$ , similar formulas for calculating the channel values at pilot positions for each separate channel can be obtained. That is, the channel values at pilot subcarriers for Rx antenna 0 is given by (11), and those for Rx antenna 1 are analogously obtained by the following equations:

$$\begin{aligned}
\mathbf{H}_{k_p,2l}(1,0) &= \frac{\mathbf{R}_{k_p,2l}(1)[\mathbf{S}_{k_p,2l}(1)]^* - \mathbf{R}_{k_p,2l+1}(1)\mathbf{S}_{k_p,2l+1}(1)}{\mathbf{S}_{k_p,2l}(0)[\mathbf{S}_{k_p,2l}(1)]^* + \mathbf{S}_{k_p,2l+1}(1)[\mathbf{S}_{k_p,2l+1}(0)]^*} \\
\mathbf{H}_{k_p,2l}(1,1) &= \frac{\mathbf{R}_{k_p,2l}(1)[\mathbf{S}_{k_p,2l+1}(0)]^* + \mathbf{R}_{k_p,2l+1}(1)\mathbf{S}_{k_p,2l}(0)}{\mathbf{S}_{k_p,2l}(0)[\mathbf{S}_{k_p,2l}(1)]^* + \mathbf{S}_{k_p,2l+1}(1)[\mathbf{S}_{k_p,2l+1}(0)]^*}
\end{aligned} \tag{13}$$

After calculating (11) and (13) to have channel values at pilot locations, the same channel estimation process as SISO approach can be utilized to estimate all the channel values at data positions. The original signal can be recovered by:

*For Alamouti 2x1:*

$$\begin{aligned}
\mathbf{S}_{2l}^{est} &= [\mathbf{H}^{est}(0,0)]^* \mathbf{R}_{2l}(0) + \mathbf{H}^{est}(0,1)[\mathbf{R}_{2l+1}(0)]^* \\
\mathbf{S}_{2l+1}^{est} &= [\mathbf{H}^{est}(0,1)]^* \mathbf{R}_{2l}(0) - \mathbf{H}^{est}(0,0)[\mathbf{R}_{2l+1}(0)]^*
\end{aligned} \tag{14}$$

*For Alamouti 2x2:*

$$\begin{aligned}
\mathbf{S}_{2l}^{est} &= [\mathbf{H}^{est}(0,0)]^* \mathbf{R}_{2l}(0) + \mathbf{H}^{est}(0,1)[\mathbf{R}_{2l+1}(0)]^* + [\mathbf{H}^{est}(1,0)]^* \mathbf{R}_{2l}(1) + \mathbf{H}^{est}(1,1)[\mathbf{R}_{2l+1}(1)]^* \\
\mathbf{S}_{2l+1}^{est} &= [\mathbf{H}^{est}(0,1)]^* \mathbf{R}_{2l}(0) - \mathbf{H}^{est}(0,0)[\mathbf{R}_{2l+1}(0)]^* + [\mathbf{H}^{est}(1,1)]^* \mathbf{R}_{2l}(1) - \mathbf{H}^{est}(1,0)[\mathbf{R}_{2l+1}(1)]^*
\end{aligned} \tag{15}$$

## 5 Simulation Results

### 5.1 Simulation Parameters

Simulation parameters are shown in table 1. Carrier frequency of 2.3 GHz is chosen, convolutional code CC(171\_133) with different rates is used as channel coding. For calculating the system throughput, the OFDM symbol is assumed to carry data from 4 individual users.

Two channel models recommended by ITU for mobile environments are used to investigate the system performance.

- Model 1: ITU\_Pedestrian B, speed 12 Km/h, Doppler frequency  $f_D \approx 25.56$  Hz.
- Model 2: ITU\_Vehicular A, speed 120 Km/h,  $f_D \approx 255.56$  Hz.

These channel models are time-variant frequency-selective channels in Non Line of Sight (NLoS) conditions. The Pedestrian B (Ped.B) model is more frequency selective than Vehicular A (Veh.A) due to its longer delay spread whereas Veh.A fades faster in time due to higher moving speed. Their specific parameters are given in table 2.

**Table 1.** Profile parameters for DL-PUSC

Bandwidth	8.75 MHz	FFT size	1024
Sampling factor ( $n$ )	8/7	Number of used subcarriers ( $N_{used}$ )	840
Sampling frequency	10 MHz	Sub-carrier spacing	9.77 KHz
Number of DL symbols used in simulation	48 (2 frames)	Modulation modes	QPSK 16-QAM 64-QAM
Useful symbol time ( $T_b$ )	102.4 $\mu$ s	CP ratio $G$	1/8
Guard Interval ( $T_g$ )	12.8 $\mu$ s	Carrier frequency	2.3GHz
OFDM Symbol Time ( $T_s$ )	115.2 $\mu$ s	Convolutional Coding ( $R_{FEC}$ )	1/2, 2/3, 3/4, 5/6

**Table 2.** Profiles of channel models used in simulation

<i>Model 1</i> ( <i>Ped.B</i> )	Path Power(dB)	-3.9	-4.8	-8.8	-11.9	-11.7	-27.8
	Path Delay( $\mu$ s)	0	0.2	0.8	1.2	2.3	3.7
<i>Model 2</i> ( <i>Veh.A</i> )	Path Power(dB)	-3.1	-4.1	-12.1	-13.1	-18.1	-23.1
	Path Delay( $\mu$ s)	0	0.31	0.71	1.09	1.73	2.51

## 5.2 Simulation Results

In these simulations, signal modulated with 3 different modulation modes, i.e. QPSK, 16QAM, and 64QAM, is propagated through the Ped.B and Veh.A channel models by using SISO and STBC approaches.

Fig. 5, 6, and 7 show the performance in term of Packet Error Rate (PER) versus Signal to Noise Ratio (SNR) of each modulation mode in 2 types of channel respectively. The ideal cases (perfect channel knowledge) for SISO as well as 2x2-Alamouti are presented as references.

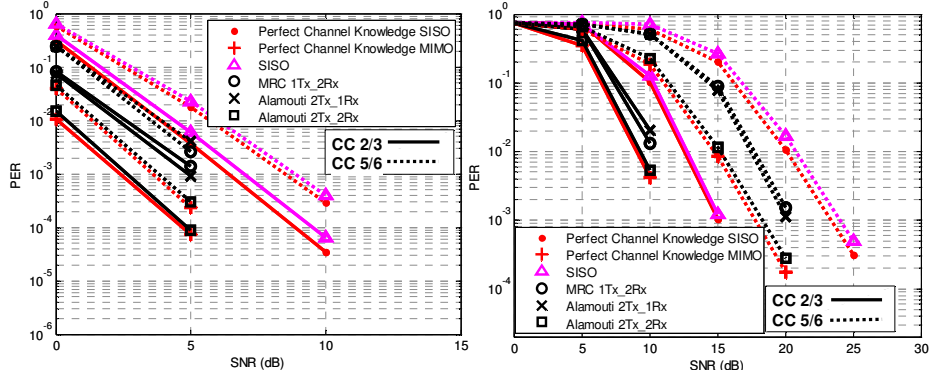


Fig. 5. PER of QPSK mode in Ped.B 12 Km/h (left) and Veh.A 120 Km/h (right).

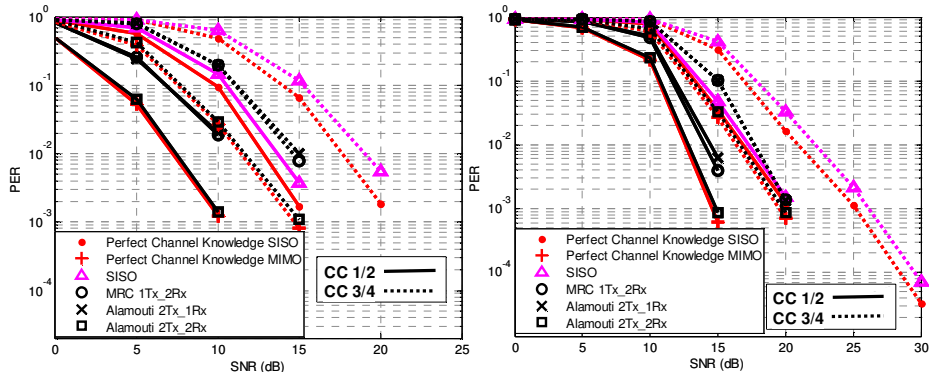


Fig. 6. PER of 16QAM mode in Ped.B 12 Km/h (left) and Veh.A 120 Km/h (right).

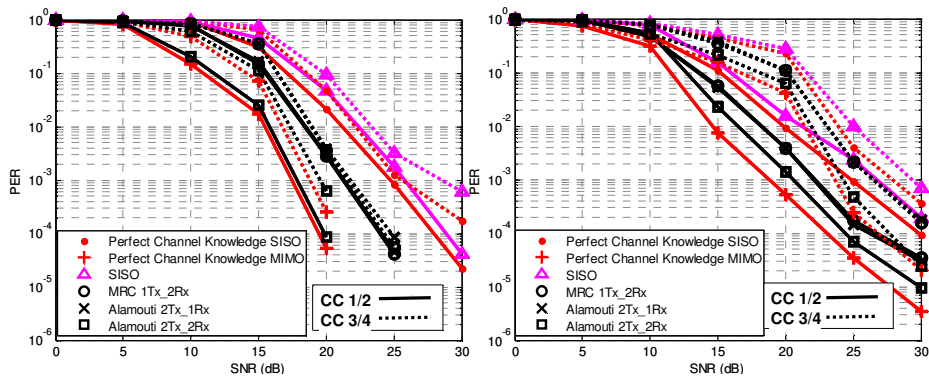


Fig. 7. PER of 64QAM mode in Ped.B 12 Km/h (left) and Veh.A 120 Km/h (right).

The results show that, in all situations, the STBC approaches always outperform the SISO scheme. The SNR gain is significantly increased from 3 to 8 dB, e.g. 64QAM at  $PER = 10^{-4}$ . Among STBC schemes, performances of MRC 1x2 and

Alamouti 2x1 are almost identical since the diversity is the same, and the transmission powers in both cases are kept equal.

Fig.8 and 9 present the comparison of the throughput (Mbps) between SISO and 2x2- Alamouti schemes. In this case the OFDM symbol is shared by 4 users. System throughput is defined in [11]. Again, it can be seen that 2x2- STBC scheme gives a remarkable improvement over the SISO approach. The gain is about 6 dB in Ped.B 12 Km/h and 4 dB in Veh.A 120 Km/h at the highest throughput (64QAM 5/6).

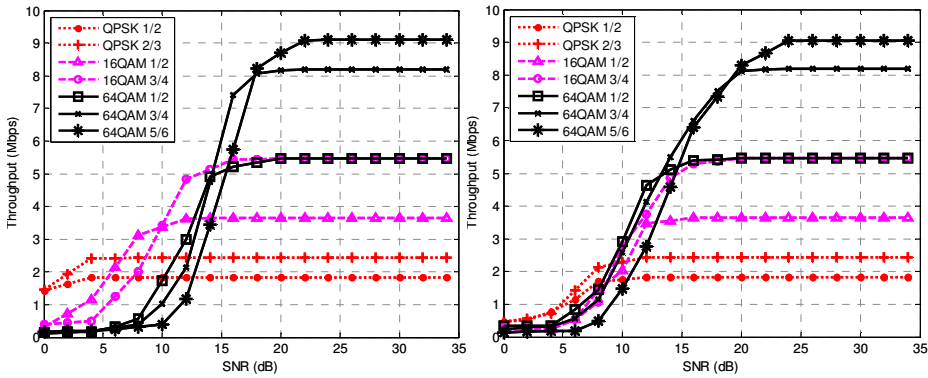


Fig. 8. SISO Throughput in Ped.B 12 Km/h (left), and Veh.A 120 Km/h (right).

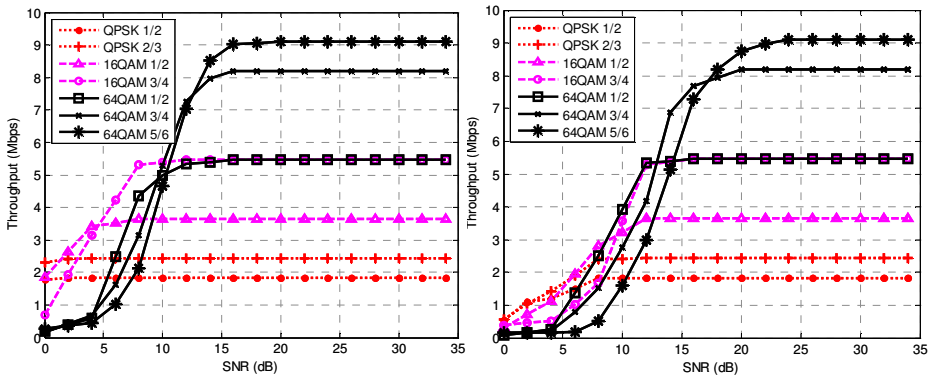


Fig. 9. 2x2- Alamouti Throughput in Ped.B 12 Km/h (left), and Veh.A 120 Km/h (right).

It should be noted that the linear interpolation method used for channel estimation works quite well thank to the pilot pattern and the cluster-size estimation. According to [14] - [15], in this setup, the Ped.B channel has a coherent time about 7.82 ms and a coherent bandwidth of 530 KHz whereas those of Veh.A model are 0.782 ms and 900 KHz respectively. From the system parameters, a cluster of 14 subcarriers covers a bandwidth of 137 KHz, and a symbol period is about 115.2 us. A block of 12 symbols, which is used for channel estimation in this simulation, spreads over 1.3824 ms of time causing a little degradation in Veh.A channel. However, in general, for this particular system, linear interpolation can ensure a good channel estimation performance.

## 6 Conclusion

In this paper, performance analysis of STBC in DL-PUSC mode of mobile WiMAX system has been presented. The system parameters are derived from the IEEE 802.16e-2005 standard. The channels used for simulation are the popular ITU pedestrian and vehicular models. Commonly used channel estimation technique is carried out to provide practical results. PER and system throughput performance comparison between SISO approach and several STBC schemes are presented. The STBC shows significant gain over the SISO approach in various channel conditions corresponding to the realistic mobile environments.

## References

1. IEEE 802.16e-2005, Part 16: Air Interface for Fixed and Mobile Broadband Wireless Access Systems, Amendment 2: Physical and Medium Access Control Layers for Combined Fixed and Mobile Operation in Licensed Bands and Corrigendum 1, (2006)
2. Ming, J., Hanzo, L.: Multiuser MIMO-OFDM for Next-Generation Wireless Systems. *Proc. of the IEEE*, vol. 95, no. 7, pp. 1430–1469, (2007)
3. Stuber, G.L., Barry, J.R., McLaughlin, S.W., Ye, L., Ingram, M.A., Pratt, T.G.: Broadband MIMO-OFDM Wireless Communications. *Proc. of the IEEE*, vol. 92, no. 2, pp. 271–294, (2004)
4. Gesbert, D., Shafi, M., Da-shan, S., Smith, P.J., Naguib, A.: From theory to practice: an overview of MIMO space-time coded wireless systems. *Journal on Selected Areas in Communications, IEEE*, vol. 21, no. 3, pp. 281–302, (2003)
5. Alamouti, S.M.: A simple transmit diversity technique for wireless communications. *Journal on Selected Areas in Communications, IEEE*, vol. 16, no. 8, pp. 1451–1458, (1998)
6. Agrawal, D., Tarokh, V., Naguib, A., Seshadri, N.: Space-time coded OFDM for high data-rate wireless communication over wideband channels. *Vehicular Technology Conference, 48th IEEE*, vol. 3, pp. 2232–2236, (1998)
7. Tarokh, V., Jafarkhani, H., Calderbank, A.R.: Space-time block codes from orthogonal designs. *IEEE Transactions on Information Theory*, vol 47, no. 5, pp. 1456–1467, (1999)
8. Hsieh, F., Fan W., Ghosh, A.: Link Performance of WiMAX PUSC. *Proc. WCNC-2008 IEEE*, pp. 1143–1148, (2008)
9. Alex, S.P., Jalloul, L.M.A.: Performance Evaluation of MIMO in IEEE802.16e/WiMAX. *Journal of Selected Topics in Signal Processing, IEEE*, vol.2, no. 2, pp. 181–190, (2008)
10. Mare, K.P., Maharaj, B.T.: Performance Analysis of Modern Space-Time Codes on a MIMO-WiMAX Platform. *Proc. WIMOB-2008. IEEE*, pp. 139–144, (2008)
11. Tran, M., Doufexi, A., Nix, A.: Mobile WiMAX MIMO performance analysis: Downlink and uplink. *Proc. 19th PIMRC-2008, IEEE*, pp 1–5, (2008)
12. Shen, Y., Martinez, E. F.: *WiMAX Channel Estimation: Algorithms and Implementations*. AN3429, Freescale Semiconductor, Inc., (2007)
13. Recommendation for ITU-R M.1225: Guidelines for evaluation of radio transmission technologies for IMT-2000. (1997)
14. Sklar, B.: Rayleigh Fading Channels in Mobile Digital Communication Systems - Part I: Characterization. *IEEE Communications Magazine*, vol. 35, no. 9, pp. 136–146, (1997)
15. Sklar, B.: Rayleigh Fading Channels in Mobile Digital Communication Systems Part II: Mitigation. *IEEE Communications Magazine*, vol. 35, no. 9, pp. 148–155, (1997)